doi: 10.4149/gpb_2019017

ROCK inhibitors alleviate myofibroblast transdifferentiation and vascular remodeling *via* decreasing TGFβ1-mediated RhoGDI expression

Jingjing Zhang[1,*], Lian Tang[1,*], Fan Dai[1], Yan Qi[1], Lifeng Yang[2], Zhaoguo Liu[1], Li Deng[3] and Wenjuan Yao[1]

[1] *Department of Pharmacology, School of Pharmacy, Nantong University, 19 QiXiu Road, Nantong, China*
[2] *Department of Pharmacy, The First People's Hospital of Changzhou, Changzhou, China*
[3] *Department of Pharmacy, Wuxi Children's Hospital, Wuxi, China*

Abstract. The aim of this study was to investigate the effects of the Rho GDP dissociation inhibitor (RhoGDI) on TGFβ1-mediated vascular adventitia myofibroblast transdifferentiation and on the inhibition of ROCK inhibitors. Myofibroblast transdifferentiation and vascular remodeling model were induced by TGFβ1 *in vitro* and by balloon injury *in vivo*. H&E (Hematoxylin & Eosin) and PSR (Picrosirius Red) staining were used to observe vascular morphology while immunofluorescence, immunohistochemistry, and Western blotting were used to measure protein expression. Fasudil treatment reduced the expression of TGFβ1, RhoGDI1, and RhoGDI2 in addition to vascular remodeling in the rat balloon injury model. TGFβ1 induced the expression of α-SMA, TGFβRI, phospho-TGFβRI, RhoGDI1, RhoGDI2, and collagen secretion in human aortic adventitial fibroblasts (HAAFs). These effects were diminished after treatment with Y27632. Suppressing both RhoGDI1 and RhoGDI2 expression also blocked TGFβ1-induced α-SMA expression and collagen secretion in HAAFs. Moreover, TGFβR inhibition blocked TGFβ1-mediated collagen secretion and the expression of α-SMA, RhoGDI1, and RhoGDI2. These data suggested that ROCK inhibitors alleviate myofibroblast transdifferentiation and vascular remodeling by decreasing TGFβ1-mediated expression of RhoGDI.

Key words: Vascular remodeling — Rho guanine nucleotide dissociation inhibitor — Rho-associated kinase — Myofibroblast — Transforming growth factor β1

Introduction

Vascular remodeling that is characterized by intima-media thickening (IMT) is the pathological basis of various vascular diseases (Zhang et al. 2015). The adventitial layer that surrounds the blood vessels has long been considered a supporting tissue that provides the muscle layers with adequate nourishment (Sartore et al. 2001). However, adventitia also play an important role in the phenotypic conversion of vascular smooth muscle cells (VSMCs), resulting in neointima formation and vascular remodeling (Faggin et al. 1999; Li et al. 2000; Sartore et al. 2001). Adventitial fibroblasts in experimental models of response to balloon vascular injury can be phenotypically converted into smooth muscle (SM)-like cells termed myofibroblasts (Wilcox and Scott 1997; Zalewski and Shi 1997). Transforming growth factor β1 (TGFβ1) is a potent driver of the differentiation of myofibroblast from fibroblasts and is accompanied by the expression of α-smooth muscle actin (α-SMA) and collagen deposition (Hinz et al. 2007). The presence of stress fibers enables the generation of higher contractile forces by myofibroblasts compared to fibroblasts and the production of overt migratory and proliferative activities in subendothelial spaces (Dunkern et al. 2007; Sun et al. 2016). Recent studies have indicated that the MEK and Smad2/3-p38MAPK-ERK1/2 pathways participate in TGF-β1-induced myofibroblast transdifferentiation in human Tenon fibroblasts (Lin et al. 2018; Wen et al. 2019). In addition, connective tissue growth factor (CTGF) is an essential downstream mediator in the TGF-β1-induced transdifferentiation of myofibroblasts

* These authors contributed equally to this work.
Correspondence to: Wenjuan Yao, Department of Pharmacology, School of Pharmacy, Nantong University, 19 QiXiu Road, Nantong 226001, Jiangsu, China
E-mail: yaowenjuan0430@aliyun.com

from Graves' orbital fibroblasts (Tsai et al. 2018). However, the molecular mechanism underlying TGFβ1-induced myofibroblast transdifferentiation in vascular adventitial fibroblasts remains unclear.

The Rho-specific guanine nucleotide dissociation inhibitor (RhoGDI) is critical for homeostasis of Rho proteins and crosstalk between Rho protein family members (Boulter and Garcia-Mata 2010). Depletion of RhoGDI1, or its yeast ortholog RDI1, can result in almost complete degradation of RhoA, Rac1, and Cdc42 proteins by proteasomes in eukaryotic cells (Boulter et al. 2010). Furthermore, numerous studies have shown that RhoGDI expression levels are associated with the presence of several cancers (Zhao et al. 2008). For example, RhoGDI1 expression is upregulated in colorectal and ovarian cancer cells, wherein high expression levels correlate with the increased invasion of cancerous cells and resistance to chemotherapy (Jones et al. 2002; Zhao et al. 2010). In contrast, RhoGDI1 expression is reduced in brain cancers and correlates with reduced expression of RhoA and RhoB, but not Rac1 proteins (Forget et al. 2002). The expression levels of RhoGDI2 also highly vary among cancers (Harding and Theodorescu 2007). However, little is known of the physiological function of RhoGDI and how RhoGDI expression is regulated. Fasudil is a Rho-associated kinase (ROCK) inhibitor that has been clinically applied and significantly contributes to the treatment of cardiovascular, neurological, and oncologic diseases (Kishi et al. 2005). Y27632 is another common ROCK inhibitor that has been extensively investigated in experimental studies (Pan et al. 2013). The inhibition of ROCK signaling pathways is associated with numerous beneficial influences in the treatment of different diseases in both research and clinical setting (Pan et al. 2013).

In the present study, an *in vivo* balloon injury-induced vascular remodeling model and an *in vitro* TGFβ1-induced myofibroblast transdifferentiation model were used to investigate the effects of ROCK inhibitors on TGFβ1-mediated RhoGDI expression, fibroblast phenotypic modulation, and vascular remodeling.

Materials and Methods

Materials

Recombinant human TGFβ1 was obtained from Novoprotein (#CA59; Shanghai, China), the TGFβ receptor inhibitor LY2109761 from Chemcatch (CC2860; Irvine, CA, USA), and the ROCK inhibitor Y27632 from Selleckchem (#129830-38-2; Houston, TX, USA). Fasudil was purchased from the Yuan Ye Biological Technology Co., Ltd. (#105628-07-7; Shanghai, China). A Fogarty 2 F balloon catheter was purchased from the Baxter Health Care Corporation (#12TLW804 F; Irvine, CA, USA). A Sirius Red staining solution kit was sourced from Solarbio (G1470; Beijing, China), while a Sirius Red collagen detection kit was purchased from Chondrex Inc. (#9062; Washington, USA). A DyLight 488-SABC SP kit was purchased from BosterBio (SA1094; Wuhan, China). A total RNA purification kit (#TR01), RevertAid first strand cDNA synthesis kit (#K1622), and DreamTaq PCR master mix (#K1071) were all purchased from Thermo Scientific (Shanghai, China). In addition, siRNAs and PCR primers were purchased from Biomics Biotechnologies (Nantong, China). RIPA lysis buffer (CW2333S) and a BCA protein assay kit (CW0014S) were both purchased from CWbio (Beijing, China), while an SDS-PAGE Gel Quick Preparation kit was sourced from Beyotime Biotechnology (P0012AC; Nantong, China). A dual-color, pre-stained protein marker was obtained from Epizyme Biological Technology (WJ101; Shanghai, China) and anti-TGFβ1 (A2124) and -RhoGDI1 (A1214) antibodies were obtained from ABclonal Technology (Wuhan, China). The antibody against phospho-TGFβRI was purchased from Sabbiotech (#12388; Maryland, USA), while the antibodies against TGFβRI (ab31013), α-SMA (ab124964), and RhoGDI2 (ab181252) were purchased from Abcam Co. (Cambridge, UK). The primary antibody against GAPDH (#5174) was obtained from Cell Signaling Technology (Beverly, MA, USA). HRP-conjugated AffiniPure Goat Anti-Rabbit IgG (H+L) was purchased from Proteintech (SA00001-2; Chicago, IL, USA) and Fluorescein (FITC)-conjugated AffiniPure Donkey Anti-Rabbit IgG (H + L) was purchased from BBI Life Sciences (D110051; Hong Kong, China). An SABC immunohistochemistry staining kit was sourced from BosterBio (SA1028; Wuhan, China). Lastly, fibroblast medium-2 (FM-2) (#2331) was purchased from ScienCell Research Laboratories (CA, USA). All other chemicals that were used in this study were of analytical grade and sourced from China.

Cell cultures and treatment

Human aortic adventitial fibroblasts (HAAFs) were purchased from ScienCell Research Laboratories (Catalog #6120; CA, USA). The cells were cultured in FM-2 medium at 37°C in a humidified incubator with a 5% CO_2 atmosphere with replacement of culture medium every three days. Cells were collected and used for experimentation from the third through seventh passages. HAAFs were first pretreated with 20 μM Y27632 for 30 min or 10 μM LY2109761 for 24 h and then exposed to 10 ng/ml TGFβ1 for 72 h.

Rat carotid artery balloon injury model

All animal experiments were performed with male Sprague-Dawley rats that were obtained from the Animal Center of Nantong University (Nantong, China) and aged 42–49 days with weights ~250 g. All animal experimental proce-

dures conformed to the NIH Guide for the Care and Use of Laboratory Animals and were approved by the Ethics Committee and the Animal Care and Use Committee of Nantong University. All animals were housed under 12 h light/dark cycles at 20°C with a humidity of 75% and received a normal diet with water *ad libitum*. Ten male rats were randomly assigned into each of three groups (n = 10/group): sham-operation, model group (balloon injury), and the fasudil-treated groups. Rat carotid artery balloon injury was established as described previously (Tulis 2007). Briefly, rats were anesthetized by an intraperitoneal injection of 4% pentobarbital, and a 2 F Fogarty balloon embolectomy catheter was introduced into the carotid artery and passed up to the aortic arch after opening of the vessel. The balloon was then inflated to distend the common carotid artery and withdrawn with rotation. Fasudil was dissolved in normal saline solution and injected intraperitoneally (30 mg/kg/d) starting the day after the operation and continuing daily for 14 days. After 14 days, the balloon-injured segment of the artery was removed, washed in saline solution on ice, and then used in subsequent experiments.

siRNA transfection

RhoGDI1 and RhoGDI2 siRNAs were used with the following sequence structure: siRhoGDI1 (sense: 5'-GUGUGGAGUACCGGAUAAAdTdT-3'; antisense: 5'-UUUAUCCGGUACUCCACACdTdT-3'), siRhoGDI2 (sense: 5'-CACAAGAGAACAAGAAUAAdTdT-3'; antisense: 5'-UUAUUCUUGUUCUCUUGUGdTdT-3'). The Lipofectamine 2000 reagent and synthetic siRNAs (20 μM in DEPC water) were diluted using Opti-MEM and then incubated at room temperature for 20 min. The mixture was added to cells, followed by incubation for 48 h. Successful interference with the target gene was then confirmed using Western blot analyses. The siRNA transfected cells were subsequently treated with 10 ng/ml TGFβ1 for 72 h.

H&E staining and Picrosirius Red (PSR) staining

The injured segments of the left common carotid arteries were isolated, fixed in 4% paraformaldehyde, and embedded in optimal cutting temperature compound (OCT). The OCT-embedded 5-μm sections were then stained with hematoxylin aqueous solution for 5 min, differentiated with hydrochloric acid for 30 s, and stained again with eosin for 2 min. The sections were then dehydrated using ethanol and cleared using xylene. The intimal area was calculated as the area of the internal elastic lamina after subtracting the luminal area. The medial area was calculated as the external elastic lamina area after subtracting the area of the internal elastic lamina area. The sections were then stained with hematoxylin aqueous solution for 10–20 min, differentiated with hydrochloric acid for 30 s, and again stained with Sirius Red solution for 1 h. The red-stained collagen was then qualified by staining intensity. All microscopy images were captured using an Olympus digital camera (Olympus, Tokyo, Japan) and analyzed using the Image-Pro Plus software program (Media Cybernetics, Rockville, MD, USA).

Picrosirius Red collagen detection

Total collagen (types I to V) content in the medium was measured using a Sirius Red collagen detection kit according to the manufacturer's instructions. Briefly, a 1× acetic acid solution was used to prepare standards and samples. A 100 μl volume of blanks, standards, and samples were added to 1.5 ml centrifuge tubes and then mixed with 500 μl of Sirius Red solution for 20 min at room temperature. All assays were performed in duplicate. The tubes were then centrifuged at 10, 000 rpm for 3 min, followed by removal of the supernatants. Pellets were washed three times with 500 μl of washing solution and then dissolved in 250 μl of extraction buffer. The solutions were transferred to 96-well plates and their absorbance was measured at 530 nm using an ELISA plate reader (BioTek Instruments, Vermont, USA).

Immunofluorescence staining

The 5-μm sections were fixed with 4% paraformaldehyde and incubated at room temperature for 60 min, followed by quenching with 5% BSA blocking buffer at 37°C for 30 min, and incubation with primary antibodies overnight at 4°C. After washing three times with PBS, the sections were incubated with anti-rabbit IgG for an additional 30 min at 37°C. Staining was then visualized using a fluorescence microscope (Olympus BX51) after DAPI staining of tissues for 20 min. Imaging was performed using an Olympus UPlanSApo 20×/0.75 objective. Hardware settings were maintained at the same levels for all experiments (FITC channel: laser power 60, exposure time 80 ms). Fluorescence intensity was quantified using the Image-Pro Plus software program. Specifically, quantification of fluorescence was calculated after conversion of the standardized pictures taken with the fluorescence microscope into 8-bit gray-scale images.

Immunohistochemistry

Immunohistochemical staining against TGFβ1 and a-SMA were performed using a strept avidin-biotin complex (SABC) immunohistochemistry staining kit and following the manufacturer's instructions. HAAFs grown on glass coverslips were washed with PBS and fixed with 4% paraformaldehyde for 20 min. The sections were allowed to equilibrate to room temperature and were then fixed with 4% paraformaldehyde for 60 min. The cells or sections were then incubated with a mix-

ture of 30% H_2O_2 and methanol for 15 min and blocked for 30 min at room temperature with PBS buffer containing 5% BSA buffer. After overnight incubation at 4°C with primary antibodies, the samples were incubated with biotinylated anti-rabbit IgG for 2 h and SABC for 1 h. The samples were then visualized using a diaminobenzidine (DAB) staining kit followed by counterstaining with hematoxylin in order to stain the target proteins brown. All images were captured using an Olympus digital camera (Olympus, Tokyo, Japan) and analyzed using the Image-Pro Plus software program (Media Cybernetics, Rockville, MD, USA).

Western blot

To conduct Western blot analyses, cells were washed with PBS and transferred to microcentrifuge tubes on ice. Then, 30–40 µl of lysis buffer (RIPA, 1 mM PMSF) was added to the cell solutions. After incubation for 40 min, the lysates were centrifuged at 12, 000 rpm for 15 min and at 4°C. Stainless steel beads were then added to the arteries for tissue protein extraction, followed by the addition of 160 µl of lysis buffer (RIPA, 1 mM PMSF). Incubation on the ice was conducted for 40 min, followed by centrifugation at 12000 r/min for 15 min at 4°C. Protein concentrations were then measured using Bradford assays. The protein samples were then separated by SDS-PAGE (polyacrylamide gel electrophoresis) and transferred to nitrocellulose membranes. The membranes were blocked for 2 h at room temperature with 5% non-fat milk in TBS (pH 7.4) containing 0.1% Tween-20. After blocking, samples were incubated with different primary antibodies overnight at 4°C and HRP-conjugated secondary antibodies for 2 h at room temperature. The blots were then visualized with an ECL detection system (Amersham Biosciences) using GAPDH as an internal standard. Relative signal intensities of the signals were quantified using densitometry and Imaging software from Labworks.

Statistical analysis

All data are presented as means ± SD. Statistical significance of differences were evaluated by one-way analyses of variance (ANOVA) followed by Tukey's post-hoc tests in the SPSS 22.0 program. Statistical significance was considered as $p < 0.05$.

Results

ROCK inhibitors reduce vascular remodeling and myofibroblast transdifferentiation by decreasing TGFβ1 expression and TGFβRI activation

The effects of fasudil on vascular remodeling were evaluated *in vivo* using a rat balloon injury model. Balloon injury resulted in obvious vascular remodeling and collagen production, as evinced by H&E and PSR staining, intima/media area ratios (0.17 ± 0.03 *vs.* 0.33 ± 0.06, $p < 0.05$), and higher collagen contents (28.24 ± 3.10 *vs.* 89.52 ± 10.11, $p < 0.01$) (Fig. 1A). In particular, fasudil treatment significantly reduced neointima formation and collagen secretion, as indicated by a 36% decrease in the intima/media area ratio and a 66% estimated reduction in collagen content. These results suggest that ROCK inhibition can effectively reverse vascular remodeling and collagen production. Further, immunohistochemistry and Western blot assays indicated that treatment with fasudil reduced TGFβ1 expression in rat carotid arteries after balloon injury (Figs. 1B and C). TGFβ1 is one of the most important regulators involved in the pathogenesis of cardiovascular diseases like restenosis following angioplasty and atherosclerosis (Verrecchia and Mauviel 2002). Consequently, the effects of ROCK inhibition on TGFβ1-induced myofibroblast transdifferentiation were evaluated *in vitro*. TGFβ1 significantly induced expression of α-SMA in HAAF cells and the secretion of collagen into medium (Figs. 1D, E and F), while these effects were inhibited by Y27632 treatment. The inhibition of TGFβ1-induced SMA expression by Y27632 is consistent with previous investigations (Ji et al. 2014). Furthermore, Y27632 treatment dramatically decreased TGFβ1-induced expression and phosphorylation of TGFβRI (Fig. 1G). Together, these data suggested that ROCK inhibition may reduce myofibroblast transdifferentiation and vascular remodeling by suppressing TGFβ1/TGFβRI activation.

ROCK inhibitors decrease RhoGDI expression in TGFβ1--induced HAAFs and balloon injury models

To clarify the role of RhoGDI in myofibroblast transdifferentiation in response to TGFβ1, the expression of both RhoGDI1 and RhoGDI2 was evaluated using Western blot analyses. RhoGDI1 and RhoGDI2 expression was significantly elevated by TGFβ1 treatment compared to the control group (Fig. 2A). In contrast, Y27632 treatment significantly decreased both RhoGDI1 and RhoGDI2 expression in TGFβ1-treated HAAFs. Further, immunostaining assay and Western blot analyses demonstrated that treatment with fasudil reduced RhoGDI1 and RhoGDI2 expression in rat carotid arteries after balloon injures (Figs. 2B and C). These results are consistent with those of the *in vitro* investigation and suggest that ROCK inhibition may reduce vascular remodeling by inhibiting RhoGDI expression.

The TGFβ receptor participates in TGFβ1-induced RhoGDI expression and myofibroblast transdifferentiation

To further elucidate the role of RhoGDI in TGFβ1-mediated myofibroblast transdifferentiation, the expression of RhoGD

was suppressed using siRNA. Suppression of both RhoGDI1 and RhoGDI2 expression significantly inhibited TGFβ1-induced α-SMA expression and collagen secretion (Figs. 3A–E), suggesting that RhoGDI was indeed involved in TGFβ1-mediated myofibroblast transdifferentiation. To assess whether TGFβ1 stimulates RhoGDI expression *via* its receptor, cells were incubated with the TGFβ receptor inhibitor LY2109761, and RhoGDI expression was measured. The

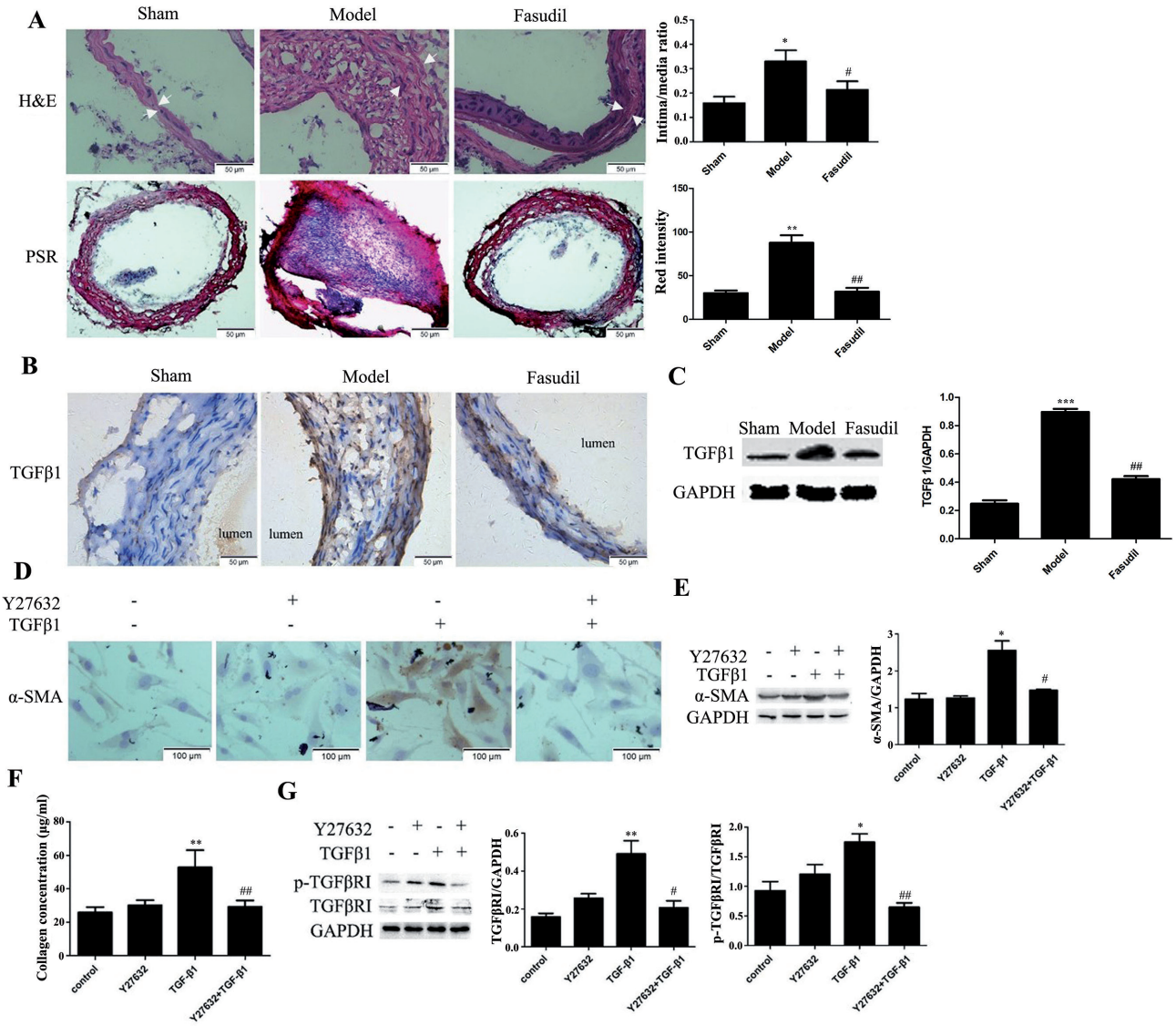

Figure 1. The effects of ROCK inhibitors on vascular remodeling and myofibroblast transdifferentiation. **A.** H&E and PSR staining of arteries 14 days after balloon injury. Rats without balloon injury were used as the sham treatment group. Arrows indicate internal and external elastic lamina, while histograms show the intima-media area ratios and the collagen (red stained) intensity. * $p < 0.05$ and ** $p < 0.01$ *vs.* the sham treatment group; # $p < 0.05$ and ## $p < 0.01$ *vs.* the injury model group ($n = 10$). **B.** Immunohistochemistry staining of TGFβ1, wherein positive staining is indicated by brown coloration and nuclei were stained with hematoxylin in blue. **C.** Western blot showing TGFβ1 expression. Histogram shows the ratio of TGFβ1 to GAPDH. *** $p < 0.001$ *vs.* the sham operation group; ## $p < 0.01$ *vs.* the injury model group ($n = 10$). **D.** Immunohistochemistry staining of α-SMA in HAAFs. Cells were pretreated with 20 μM Y27632 for 30 min and then exposed to 10 ng/ml TGFβ1 for an additional 72 h. Untreated cells were used as controls. α-SMA-positive cells are indicated by brown coloration. **E.** Western blot showing the expression of α-SMA. Histogram shows the ratio of α-SMA to GAPDH. * $p < 0.05$ *vs.* the control group; # $p < 0.05$ *vs.* the TGFβ1-treated group ($n = 3$). **F.** Detection of collagen secretion into media. Histogram shows collagen concentrations in each group based on absorbance at 530 nm. ** $p < 0.01$ *vs.* the control group; ## $p < 0.01$ *vs.* the TGFβ1-treated group ($n = 3$). **G.** Western blot showing the expression of TGFβRI and phospho-TGFβRI. Histograms show the ratio of expression levels of phospho-TGFβRI to TGFβRI or TGFβRI to GAPDH. * $p < 0.05$, ** $p < 0.01$ *vs.* the control group; # $p < 0.05$ and ## $p < 0.01$ *vs.* the TGFβ1-treated group ($n = 3$). (See online version for color figure.)

expression levels of RhoGDI1 and RhoGDI2 were significantly decreased after LY2109761 incubation in the TGFβ1 treatment group (Fig. 3F), suggesting that TGFβ1 stimulates RhoGDI expression through TGFβ receptor activation. The effects of TGFβ receptor inhibition on TGFβ1-induced cell transdifferentiation were also evaluated and revealed that LY2109761 pretreatment clearly suppressed TGFβ1-induced α-SMA expression and collagen secretion (Figs. 3G–I).

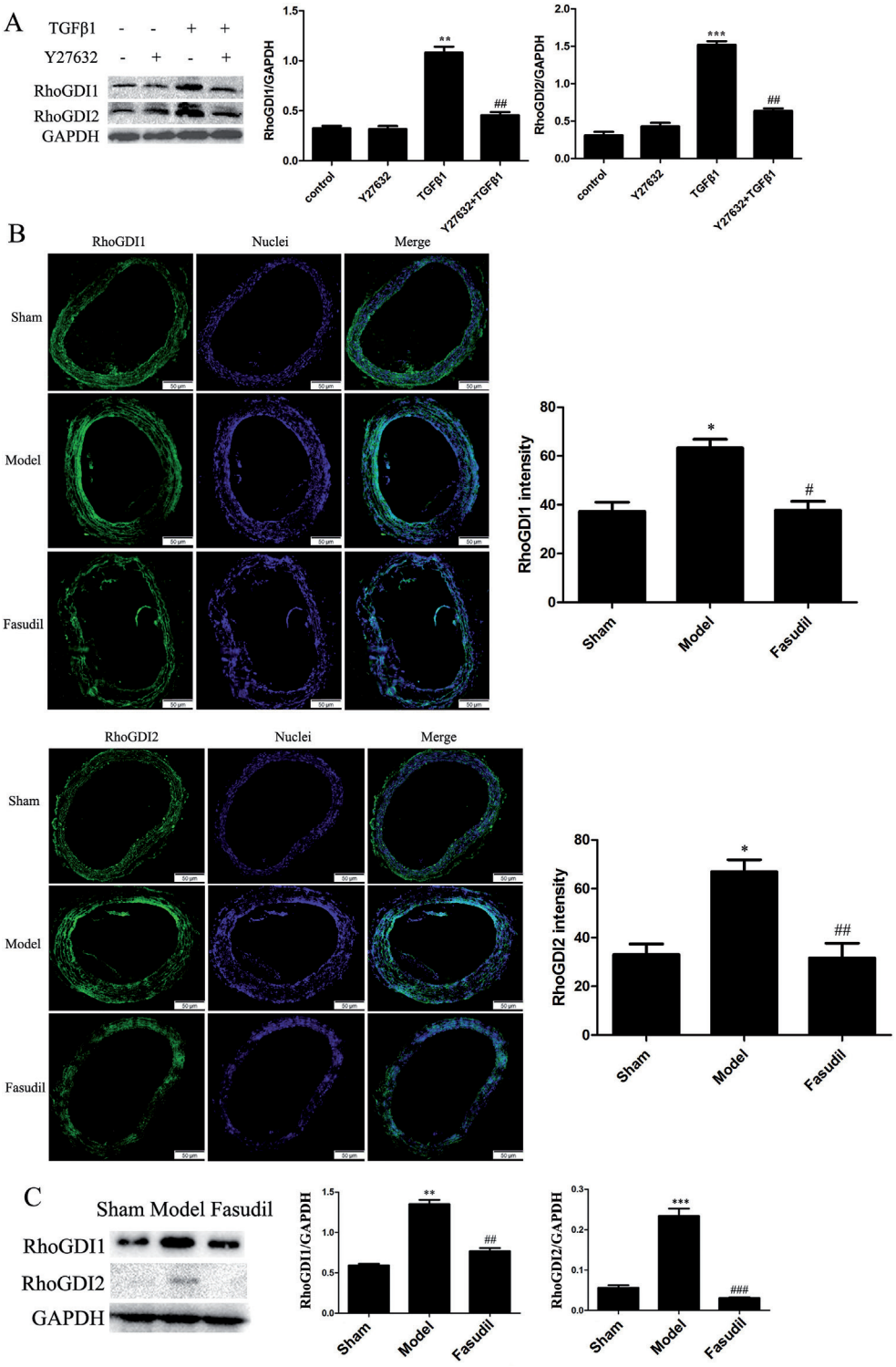

Figure 2. The effect of ROCK inhibition on RhoGDI expression. **A.** Western blot showing the expression of RhoGDI1 and RhoGDI2. Cells were pretreated with 20 μM Y27632 for 30 min and then exposed to 10 ng/ml TGFβ1 for an additional 72 h. Untreated cells were used as the control group. Histograms show the ratio of RhoGDI1 or RhoGDI2 to GAPDH. ** $p < 0.01$ and *** $p < 0.001$ *vs.* the control group; ## $p < 0.01$ *vs.* the TGFβ1-treated group ($n = 3$). **B.** Immunofluorescence staining of RhoGDI1 and RhoGDI2 (shown in green), with nuclei stained with DAPI in blue. Histograms show the fluorescence intensity of staining. Rats without balloon injury were used as the sham operation group. * $p < 0.05$ *vs.* the sham operation group; # $p < 0.05$ and ## $p < 0.01$ *vs.* the injury model group ($n = 10$). **C.** Western blot showing RhoGDI1 and RhoGDI2 expression after balloon injury. Rats without balloon injury were used as the sham operation group. Histograms show the ratio of RhoGDI1 or RhoGDI2 to GAPDH. ** $p < 0.01$ and *** $p < 0.001$ *vs.* the sham operation group; ## $p < 0.01$ and ### $p < 0.001$ *vs.* the injury model group ($n = 10$). (See online version for color figure.)

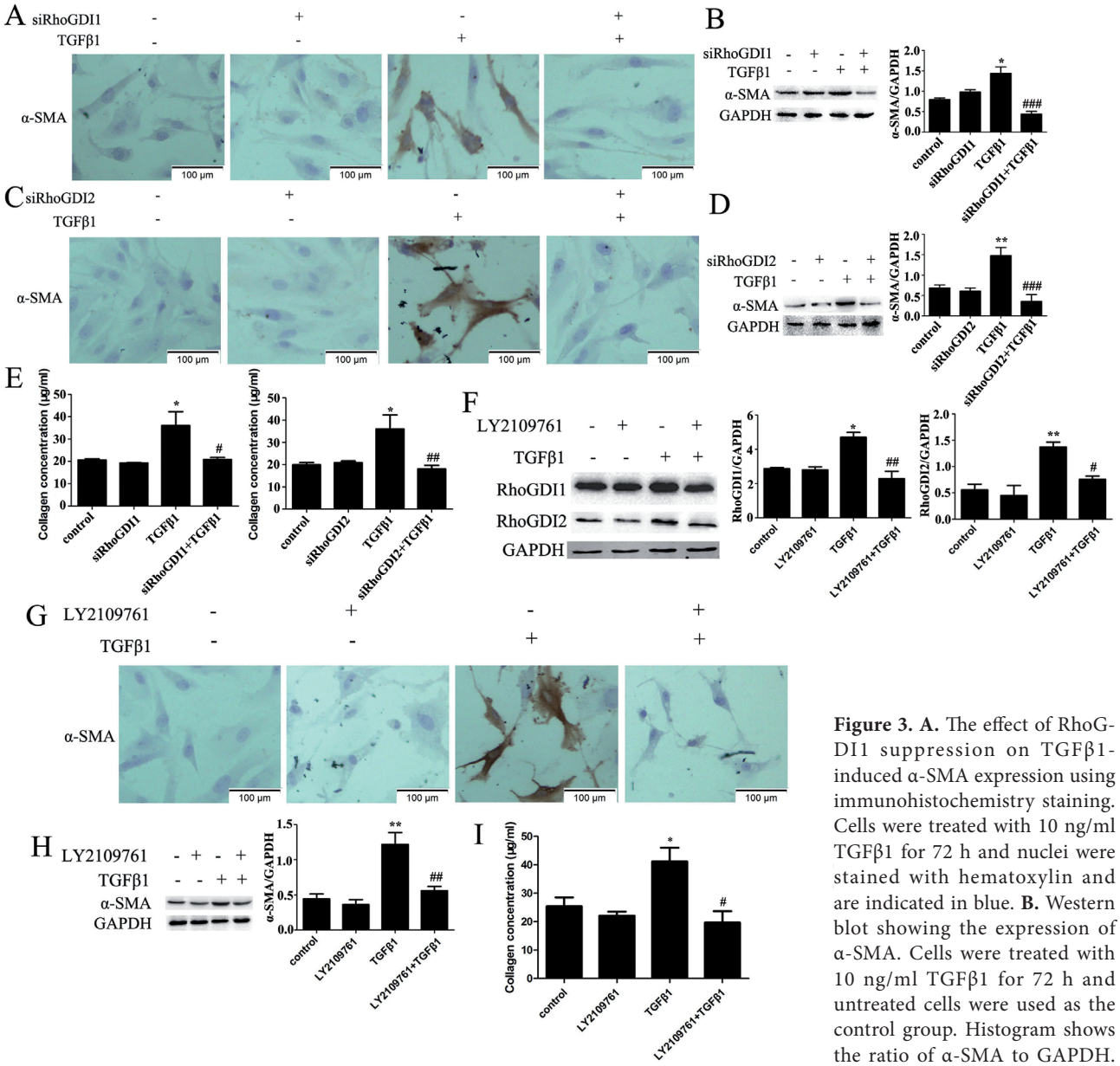

Figure 3. A. The effect of RhoGDI1 suppression on TGFβ1-induced α-SMA expression using immunohistochemistry staining. Cells were treated with 10 ng/ml TGFβ1 for 72 h and nuclei were stained with hematoxylin and are indicated in blue. **B.** Western blot showing the expression of α-SMA. Cells were treated with 10 ng/ml TGFβ1 for 72 h and untreated cells were used as the control group. Histogram shows the ratio of α-SMA to GAPDH. * $p < 0.05$ *vs.* the control group; ### $p < 0.001$ *vs.* the TGFβ1-treated group ($n = 3$). **C.** The effect of RhoGDI2 suppression on TGFβ1-induced α-SMA expression using immunohistochemistry staining. Nuclei were stained with hematoxylin and are indicated in blue. **D.** Western blot showing α-SMA expression. Cells were treated with 10 ng/ml TGFβ1 for 72 h and untreated cells were used as the control group. Histogram shows the ratio of α-SMA to GAPDH. ** $p < 0.01$ *vs.* the control group; ### $p < 0.001$ *vs.* the TGFβ1-treated group ($n = 3$). **E.** The effect of RhoGDI suppression on TGFβ1-induced collagen secretion using Sirius Red Collagen Detection Kit. Histograms show the concentrations of collagen in each group, indicated by absorbance values at 530 nm. Untreated cells were used as the control group. * $p < 0.05$ *vs.* the control group; # $p < 0.05$ and ## $p < 0.01$ *vs.* the TGFβ1-treated group ($n = 3$). **F.** The effect of LY2109761 pretreatment on the expression of RhoGDI. Cells were pretreated with 10 μM LY2109761 for 24 h and then exposed to 10 ng/ml TGFβ1 for 72 h. Cells without treatment was used as the control group. Histograms show the ratio of RhoGDI1 or RhoGDI2 to GAPDH. * $p < 0.05$ and ** $p < 0.01$ *vs.* the control group; # $p < 0.05$ and ## $p < 0.01$ *vs.* the TGFβ1-treated group ($n = 3$). **G.** Immunohistochemistry determination of α-SMA expression. Nuclei were stained with hematoxylin and are shown in blue. **H.** Western blot showing α-SMA expression. Histogram shows the ratio of α-SMA to GAPDH. ** $p < 0.01$ *vs.* the control group; ## $p < 0.01$ *vs.* the TGFβ1-treated group ($n = 3$). **I.** The effect of LY2109761 pretreatment on TGFβ1-induced collagen secretion. Histogram shows the concentrations of collagen in each group. Untreated cells were used as the control group. * $p < 0.05$ *vs.* the control group; # $p < 0.05$ *vs.* the TGFβ1-treated group ($n = 3$). (See online version for color figure.)

Discussion

Vascular remodeling is a common pathophysiological process following cardiovascular diseases like atherosclerosis and hypertension. Consequently, investigation of myofibroblast transdifferentiation in vascular adventitial fibroblasts has become increasingly important for understanding vascular remodeling mechanisms. RhoGDIs are important physiological regulators that belong to the Rho family of small GTPases. An emerging body of literature suggests that their activity is altered during carcinogenesis and tumor progression (Boulter et al. 2010). However, the effects of RhoGDI on myofibroblast phenotypic modulation and vascular remodeling are not well understood. Indeed, this is the first study to report that RhoGDI participates in TGFβ1-mediated myofibroblast transdifferentiation and vascular remodeling, and also the first to investigate the inhibitory effects of ROCK inhibitors.

Our results demonstrated that TGFβ1 promotes RhoGDI1 and RhoGDI2 expression by activating the TGFβ receptor in TGFβ1-induced HAAF cells *in vitro* and *via* the same pathway in an *in vivo* balloon injury model. In addition, the suppression of RhoGDI and inhibition of the TGFβ receptor significantly decreased TGFβ1-induced α-SMA expression and collagen secretion in HAAFs. These observations suggested that RhoGDI affects the phenotypic modulation of TGFβ1-induced myofibroblast *via* the TGFβ receptor. ROCK Inhibition has been previously shown to exhibit therapeutic benefits for a variety of diseases. Y27632 and fasudil are the most well-known ROCK inhibitors, and have been used extensively in previous experiments (Pan et al. 2013). Here, fasudil treatment resulted in decreases in the expression of TGFβ1, neointima formation, and collagen production in an *in vivo* rat balloon injury model. In addition, Y27632 treatment inhibited TGFβ1-mediated myofibroblast transdifferentiation and the expression and activation of TGFβ receptors. These results suggested that ROCK inhibitors reduce myofibroblast transdifferentiation and vascular remodeling by regulating TGFβ1 and its downstream pathways. Moreover, ROCK inhibition reduced levels of both RhoGDI1 and RhoGDI2 in an *in vivo* balloon injury model and an *in vitro* model of TGFβ1-induced HAAF differentiation. In summary, the primary findings of this study are that: (1) RhoGDI expression is involved in regulating myofibroblast phenotypic modula-

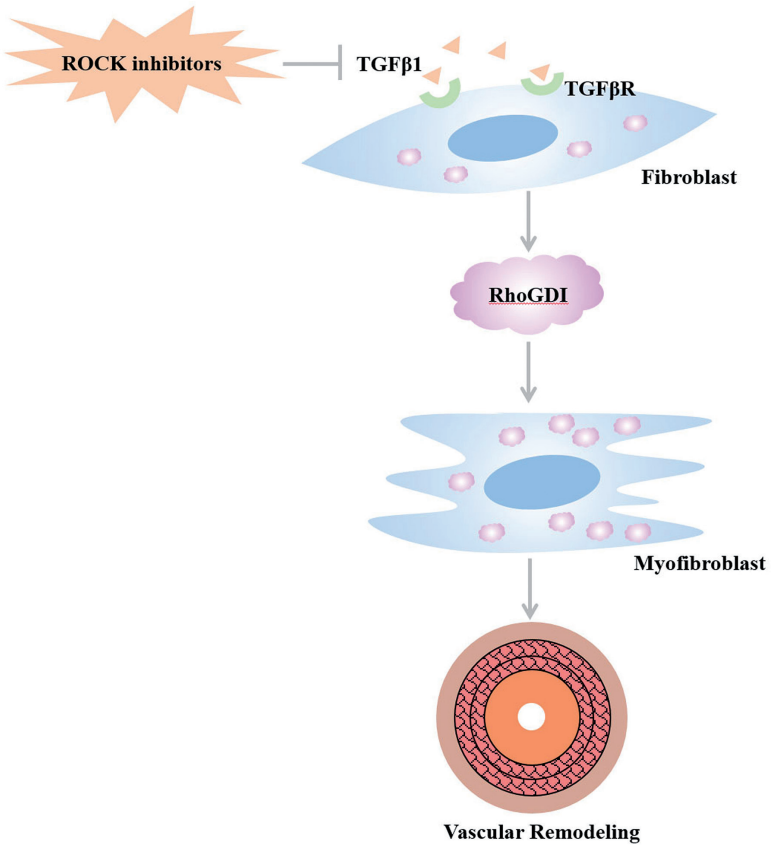

Figure 4. Diagram of the effects of ROCK inhibitors on TGFβ1-mediated RhoGDI expression, myofibroblast transdifferentiation and vascular remodeling.

tion and vascular remodeling as mediated by TGFβ1 and its receptor; and (2) ROCK inhibitors inhibit TGFβ1-induced myofibroblast transdifferentiation and vascular remodeling by regulating the activity of the TGFβ1/RhoGDI pathway (Fig. 4).

Conflict of interest. The authors have no conflicts of interest to declare in relation to this article.

Acknowledgments. This work was supported by grants from the National Natures Science Foundation of Nantong City (No. JC2018059), the Jiangsu Planned Projects for Postdoctoral Research Funds (No. 1601107C) and the National Natural Science Foundation of China (No. 81703884).

References

Boulter E, Garcia-Mata R, Guilluy C, Dubash A, Rossi G, Brennwald PJ, Burridge K (2010): Regulation of Rho GTPase crosstalk, degradation and activity by RhoGDI1. Nat. Cell. Biol. **12,** 477-483 https://doi.org/10.1038/ncb2049

Boulter E, Garcia-Mata R (2010): RhoGDI: A rheostat for the Rho switch. Small GTPases **1,** 65-68 https://doi.org/10.4161/sgtp.1.1.12990

Dunkern TR, Feurstein D, Rossi GA, Sabatini F, Anathematize A (2007): Inhibition of TGF-β induced lung fibroblast to myofibroblast conversion by phosphodiesterase inhibiting drugs and activators of soluble guanylyl cyclase. Eur. J. Pharmacol. **572,** 12-22 https://doi.org/10.1016/j.ejphar.2007.06.036

Faggin E, Puato M, Zardo L, Franch R, Millino C, Sarinella F, Pauletto P, Sartore S, Chiavegato A (1999): Smooth muscle-specific SM22 protein is expressed in the adventitial cells of the balloon-injured rabbit carotid artery. Arterioscler. Thromb. Vasc. Biol. **19,** 1393-1404 https://doi.org/10.1161/01.ATV.19.6.1393

Forget MA, Desrosiers RR, Del M, Moumdjian R, Shedid D, Berthelet F, Beliveau R (2002): The expression of rho proteins decreases with human brain tumor progression: potential tumor markers. Clin. Exp. Metastasis **19,** 9-15 https://doi.org/10.1023/A:1013884426692

Harding MA, Theodorescu D (2007): RhoGDI2: a new metastasis suppressor gene: discovery and clinical translation. Urol. Oncol. **25,** 401-406 https://doi.org/10.1016/j.urolonc.2007.05.006

Hinz B, Phan SH, Thannickal VJ, Galli A, Bochaton-Piallat M, Gabbiani G (2007): The myofibroblast: one function, multiple origins. Am. J. Pathol. **170,** 1807-1816 https://doi.org/10.2353/ajpath.2007.070112

Jones MB, Krutzsch H, Shu H, Zhao Y, Liotta LA, Kohn EC, Petricoin EF (2002): Proteomic analysis and identification of new biomarkers and therapeutic targets for invasive ovarian cancer. Proteomics **2,** 76-84 https://doi.org/10.1002/1615-9861(200201)2:1<76::AID-PROT76>3.0.CO;2-O

Ji H, Tang H, Lin H, Mao J, Gao L, Liu J, Wu T (2014): Rho/Rock cross-talks with transforming growth factor-β/Smad pathway participates in lung fibroblast-myofibroblast differentiation. Biomed. Rep. **2,** 787-792 https://doi.org/10.3892/br.2014.323

Kishi T, Hirooka Y, Masumoto A, Ito K, Kimura Y, Inokuchi K, Tagawa T, Shimokawa H, Takeshita A, Sunagawa K (2005): Rho-kinase inhibitor improves increased vascular resistance and impaired vasodilation of the forearm in patients with heart failure. Circulation **111,** 2741-2747 https://doi.org/10.1161/CIRCULATIONAHA.104.510248

Li G, Chen SJ, Oparil S, Chen YF, Thompson JA (2000): Direct in vivo evidence demonstrating neointimal migration of adventitial fibroblasts after balloon injury of rat carotid artery. Circulation **101,** 1362-1365 https://doi.org/10.1161/01.CIR.101.12.1362

Lin X, Wen J, Liu R, Gao W, Qu B, Yu M (2018): Nintedanib inhibits TGF-β-induced myofibroblast transdifferentiation in human Tenon's fibroblasts. Mol. Vis. **24,** 789-800

Pan P, Shen M, Yu H, Li Y, Li D, Hou T (2013): Advances in the development of Rho-associated protein kinase (ROCK) inhibitors. Drug. Discov. Today **18,** 1323-1333 https://doi.org/10.1016/j.drudis.2013.09.010

Sartore S, Chiavegato A, Faggin E, Franch R, Puato M, Ausoni S, Pauletto P (2001): Contribution of adventitial fibroblasts to neointima formation and vascular remodeling: from innocent bystander to active participant. Circ. Res. **89,** 1111-1121 https://doi.org/10.1161/hh2401.100844

Sun YB, Qu X, Caruana G, Li J (2016): The origin of renal fibroblasts/myofibroblasts and the signals that trigger fibrosis. Differentiation **92,** 102-107 https://doi.org/10.1016/j.diff.2016.05.008

Tsai CC, Wu SB, Kau HC, Wei YH (2018): Essential role of connective tissue growth factor (CTGF) in transforming growth factor-β1 (TGF-β1)-induced myofibroblast transdifferentiation from Graves' orbital fibroblasts. Sci. Rep. **8,** 7276 https://doi.org/10.1038/s41598-018-25370-3

Tulis DA (2007): Rat carotid artery balloon injury model. Methods. Mol. Med. **139,** 1-30 https://doi.org/10.1007/978-1-59745-571-8_1

Verrecchia F, Mauviel A (2002): Transforming growth factor-β signaling through the Smad pathway: role in extracellular matrix gene expression and regulation. J. Invest. Dermatol. **118,** 211-215 https://doi.org/10.1046/j.1523-1747.2002.01641.x

Wen J, Lin X, Gao W, Qu B, Ling Y, Liu R, Yu M (2019) MEK inhibition prevents TGFβ1 induced myofibroblast transdifferentiation in human tenon fibroblasts. Mol. Med. Rep. **19,** 468-476 https://doi.org/10.3892/mmr.2018.9673

Wilcox JN, Scott NA (1997): Potential role of the adventitia in arteritis and atherosclerosis. Int. J. Cardiol. **54,** (Suppl.), S21-S35 https://doi.org/10.1016/S0167-5273(96)02811-2

Zalewski A, Shi Y (1997): Vascular myofibroblasts: lessons from coronary repair and remodeling. Arterioscler. Thromb. Vasc. Biol. **17,** 417-422 https://doi.org/10.1161/01.ATV.17.3.417

Zhao L, Wang H, Li J, Liu Y, Ding Y (2008): Overexpression of Rho GDP-dissociation inhibitor alpha is associated with tumor progression and poor prognosis of colorectal cancer. J. Proteome. Res. **7,** 3994-4003

https://doi.org/10.1021/pr800271b
Zhao L, Wang H, Sun X, Ding Y (2010): Comparative proteomic analysis identifies proteins associated with the development and progression of colorectal carcinoma. FEBS J. **277,** 4195-4204
https://doi.org/10.1111/j.1742-4658.2010.07808.x
Zhang XY, Zhang T, Gao F, Li QL, Shen CY, Li YK, Li W, Zhang XM (2015): Fasudil, a Rho-kinase inhibitor, prevents intima-media thickening in a partially ligated carotid artery mouse model: Effects of fasudil in flow-induced vascular remodeling. Mol. Med. Rep. **12,** 7317-7325
https://doi.org/10.3892/mmr.2015.4409

Received: March 3, 2019
Final version accepted: May 7, 2019
First published online: June 20, 2019